Optical Feshbach resonances through a molecular dark state: Efficient manipulation of *p*-wave resonances in fermionic ^{171}Yb atoms

Subrata Saha,[1] Arpita Rakshit,[1] Debashree Chakraborty,[1] Arpita Pal,[1] and Bimalendu Deb[1,2]
[1]*Department of Materials Science, Indian Association for the Cultivation of Science, Jadavpur, Kolkata 700032, India*
[2]*Raman Centre for Atomic, Molecular and Optical Sciences, Indian Association for the Cultivation of Science, Jadavpur, Kolkata 700032, India*
(Received 15 May 2014; published 1 July 2014)

In a recent experiment by Yamazaki *et al.* [Phys. Rev. A **87**, 010704(R) (2013)], a *p*-wave optical Feshbach resonance in fermionic ^{171}Yb atoms using purely long-range molecular excited states has been demonstrated. We show theoretically that, if two purely long-range excited states of ^{171}Yb are coupled to the ground-state continuum of scattering states with two lasers, then it is possible to significantly suppress photoassociative atom loss by a dark resonance in the excited states. We present a general theoretical framework for creating a dark state in an electronically excited molecular potential for the purpose of increasing the efficiency of the optical Feshbach resonance. This can be accomplished by properly adjusting the relative intensity, phase, polarizations, and frequency detunings of two lasers. We present selected numerical results for atom-loss spectra and *p*-wave elastic- and inelastic-scattering cross sections of ^{171}Yb atoms to illustrate the effects of the molecular dark state on the optical Feshbach resonance.

DOI: 10.1103/PhysRevA.90.012701 PACS number(s): 34.50.Cx, 34.50.Rk, 67.85.Lm

I. INTRODUCTION

The ability to control interparticle interactions is important for exploring the fundamental physics of many-particle systems in various interaction regimes. Toward this end, ultracold atomic gases offer unique opportunities since atom-atom interaction at low energy can be manipulated with external fields. In recent times, a magnetic Feshbach resonance (MFR) [1–3] was extensively used to tune *s*-wave scattering length a_s of atoms over a wide range, facilitating the first demonstration of *s*-wave fermionic superfluidity in an atomic Fermi gas [4]. A *p*-wave MFR was experimentally observed in spin polarized ^{40}K [5] and ^{6}Li [6,7] atomic gases, and analyzed theoretically [8,9]. MFR was used to produced *p*-wave Feshbach molecules [10,11]. Atom-atom interactions can also be altered by an optical Feshbach resonance (OFR), as proposed by Fedichev *et al.* [12]. The tunability of a_s by an OFR was demonstrated experimentally [13–15], albeit for a limited range. Recently, Yamazaki *et al.* [16] demonstrated experimentally a *p*-wave OFR in fermionic ^{171}Yb atoms following an earlier theoretical proposal by Goel *et al.* [17].

In an OFR, a photoassociation (PA) laser is used to couple the scattering or free state of two *S* (ground) atoms to a bound state in an excited molecular potential asymptotically connecting to one ground (*S*) and another excited (*P*) atom. The loss of atoms due to spontaneous emission from the excited bound state is a severe hindrance to efficient manipulation of atom-atom interactions by an optical method. In the dispersive regime, the magnitude of the free-bound detuning is larger than both the spontaneous and stimulated linewidths. In this regime, although the atom loss is mitigated, the change in elastic scattering amplitude is small. On the other hand, if the laser is tuned close to the free-bound transition frequency, there will be a photoassociative formation of excited molecules which will eventually decay, leading to a drastic loss of atoms from the trap. Until now it has been found that OFR is not an efficient method for tuning a_s, as compared with MFR. It is therefore important to devise new methods to increase the efficiency of OFRs. By using an OFR, one can manipulate not only *s*-wave but also higher-partial-wave interactions [18,19] between ultracold atoms. Apart from this, the development of an efficient OFR method is primarily necessary to manipulate two-body interactions in nonmagnetic atoms to which a MFR is not applicable. The following question then arises: Is there any way out to suppress the loss of atoms in order to coherently and all-optically manipulate atom-atom interactions? To address this, we carry out a theoretical study showing the manipulation of *p*-wave interactions in fermionic ^{171}Yb atoms by two lasers in different coupling regimes.

Here we show that it is possible to make an OFR significantly efficient by substantially suppressing atom loss by the method of dark-state resonance [20,21] in molecular excited states. Usually, a dark state resonance refers to the formation of a coherent superposition of two ground-state sublevels of an atom or a molecule by two lasers. When a dark state is formed in ground-state sublevels, an atom or a molecule cannot effectively absorb a photon to reach to an excited state, and therefore no fluorescence light comes out. Dark resonance in ground-state sublevels is well known and plays an essential role in a number of coherent phenomena such as coherent population trapping (CPT) [22], laser cooling [23,24], electromagnetically induced transparency (EIT) [21], stimulated Raman adiabatic passage (STIRAP) [25–27], slow light [28,29], etc. In contrast, dark resonances in atomic or molecular excited states have remained largely unexplored, because the excited states are, in general, too lossy. Now, with the accessibility of relatively long-lived excited states of alkaline-earth–like atoms via intercombination PA transitions [30,31], it is possible to create a coherent superposition or a coherence in rovibrational states of an excited molecule by two PA lasers. Although this laser-induced coherence was discussed earlier in the contexts of *d*-wave OFR [19], vacuum-induced coherence [32], and rotational quantum beats [33], here we give an exposition of the crucial role it can play in manipulating an OFR. When two molecular rovibrational

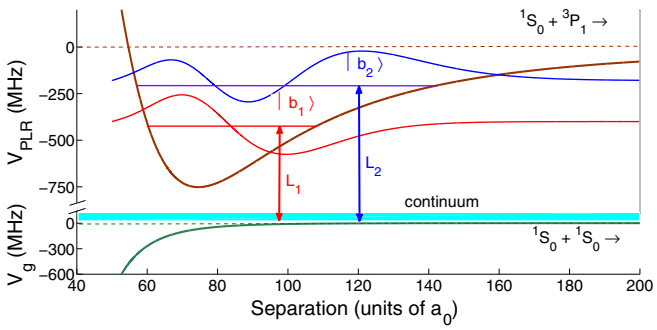

FIG. 1. (Color online) Schematic diagram for generating coherence between two PLR bound states $|b_1\rangle$ and $|b_2\rangle$ of $^{171}Yb_2$ by two OFR lasers L_1 and L_2. The ground-state potential V_g (units of MHz) and PLR potential V_{PLR} (units of MHz) are plotted against the internuclear separation in units of the Bohr radius a_0. Asymptotically, V_g corresponds to two separated atoms in electric $^1S_0 + {}^1S_0$ states while V_{PLR} connects two separated atoms in electronic $^1S_0 + {}^3P_1$ states. $|b_1\rangle$ and $|b_2\rangle$ have vibrational quantum numbers $\nu_1 = 1$ and $\nu_2 = 2$, respectively; both have the same rotational quantum number T_e equal to either 1 or 3.

states belonging to the same electronically excited potential have the same rotational but different vibrational quantum numbers, it is possible to generate a superposition of these two levels by applying two PA lasers. Under appropriate conditions, this superposed state can be protected against spontaneous emission, leading to CPT in excited states [32].

Our purpose is to make use of molecular dark resonance to control OFR. For illustration, we investigate the manipulation of the p-wave scattering properties of ^{171}Yb atoms with two OFR lasers L_1 and L_2 tuned to PA transitions to two purely-long-range (PLR) bound states $|b_1\rangle$ and $|b_2\rangle$, respectively; as shown in Fig. 1. $|b_1\rangle$ and $|b_2\rangle$ were chosen to have the same rotational quantum number $T_1 = T_2 = T_e$ but different vibrational quantum numbers $\nu_1 = 1$ and $\nu_2 = 2$, respectively. T may be chosen to be 1 or 3. By treating both lasers on an equal footing, we obtain results for any arbitrary optical-coupling regime. Our results show that the elastic-scattering rate can exceed the inelastic rate by five orders of magnitude under the molecular-dark-resonance conditions in the strong-coupling regime. The atom loss can be almost completely eliminated by the use of the dark state. This leads to the huge enhancement in the efficiency of an all-optical method for controlling atom-atom interactions.

The remainder of the paper is organized in the following way: In the next section we present our theory of two-laser OFRs, emphasizing the essential idea behind the creation and utilization of molecular dark resonances for suppressing atom loss. In Sec. III, we apply this theoretical method to manipulate p-wave interactions of ^{171}Yb atoms. We then present numerical results and interpret them in Sec. IV. The paper is concluded in Sec. V.

II. THEORY

We first give the general idea behind molecular-dark-state–assisted OFR. We then specialize our theoretical method for p-wave OFRs in fermionic ^{171}Yb atoms. A scheme of two-laser OFR in ^{171}Yb is depicted in Fig. 1, which may also be used for a general scheme of two-laser OFR of ultracold atoms. Since photoassociative interactions between a nonzero partial-wave ($\ell \neq 0$) scattering state of two electronically-ground-state atoms and an excited molecular bound state is essentially anisotropic, the usual theoretical method for s-wave OFR given by Bohn and Julienne [34] needs to be extended to include anisotropic effects. In our theoretical treatment, we take into account all the magnetic sublevels of the ground and excited rotational levels. The two lasers are taken to be copropagating and linearly polarized along the z axis.

Two molecular bound states $|b_1\rangle$ and $|b_2\rangle$ supported by an excited-state potential are coupled to the continuum of unperturbed ground scattering states $|E'\rangle$ with collision energy E' by two PA lasers L_1 and L_2. This leads to the formation of energy-normalized dressed states [19]:

$$|\psi_E\rangle = A_{1E}|b_1\rangle + A_{2E}|b_2\rangle + \int dE' C_{E'}(E)|E'\rangle, \quad (2.1)$$

where A_{1E}, A_{2E}, and $C_{E'}(E)$ are the dressed amplitudes given by

$$A_{1E} = D_{1E}^{-1} e^{i\phi_{L_1}} \left[\Lambda_{1E} + \mathscr{L}_1^{(2)}\right], \quad (2.2)$$

$$A_{2E} = D_{2E}^{-1} e^{i\phi_{L_2}} \left[\Lambda_{2E} + \mathscr{L}_2^{(1)}\right], \quad (2.3)$$

$$C_{E'}(E) = \delta(E - E') + \int dE' \frac{A_{1E}\Lambda_{1E'} + A_{2E}\Lambda_{2E'}}{E - E'}, \quad (2.4)$$

where ϕ_{L_n} is the phase of laser L_n. In the expression of A_{nE}, the first term $D_{nE}^{-1}\Lambda_{nE}$ is the amplitude that depends on direct free-bound coupling Λ_{nE} between the bound state $|b_n\rangle$ and the continuum due to laser L_n, while the second term $D_{nE}^{-1}\mathscr{L}_n^{(n')}$ results from the cross coupling between the bound states by the two lasers. Here the denominator $D_{nE} = E + \hbar\tilde{\delta}_n(E) + i\hbar G_n(E)$ with $\tilde{\delta}_n$ being the detuning of laser L_n from the light-shifted nth bound state,

$$\tilde{\delta}_n = \delta_n + \frac{1}{\hbar}\left(E_{b_n}^{\text{shift}} + E_{nn'}^{\text{shift}}\right), \quad (2.5)$$

where $\delta_n = \Delta_n + E_{b_n}/\hbar$ with $\Delta_n = \omega_{L_n} - \omega_A$ being the detuning of the nth laser from the frequency of atomic transition $S \rightarrow P$, E_{b_n} is the binding energy of $|b_n\rangle$ measured from the threshold of the excited-state potential and $E_{b_n}^{\text{shift}}$ is the light shift of the bound state. Here, $G_n(E) = \Gamma_n(E) + \Gamma_{nn'}(E)$ with $\Gamma_n(E)$ being the stimulated linewidth of the nth bound state due to laser L_n, and $E_{nn'}^{\text{shift}}$ and $\Gamma_{nn'}$ are the terms that depend on the terms $\mathscr{L}_1^{(2)}$ and $\mathscr{L}_2^{(1)}$. Note that $\Gamma_{nn'}$ can be negative, but $G_n \geqslant 0$.

Equation (1) is derived without taking spontaneous emission into account. Following Bohn and Julienne [34], spontaneous decay can be included into the problem by introducing an "artificial" open channel in the ground-state manifold. Let the state of this artificial decay channel be denoted by $|E\rangle_{\text{art}}$ and let its interaction with an excited state be denoted by V_{art}. The spontaneous-emission linewidth can be identified with

$$\gamma_n = \frac{2\pi}{\hbar}|_{\text{art}}\langle E|V_{\text{art}}|b_n\rangle|^2. \quad (2.6)$$

As a result, G_n should be replaced by $G_n + \gamma_n$. The T-matrix element for the inelastic process of transitions from the two correlated excited states to $|E\rangle_{\rm art}$ is

$$\pi\,{}_{\rm art}\langle E|V_{\rm art}|\psi_E\rangle = \pi\left(\mathcal{V}_1 A_{1E} + \mathcal{V}_2 A_{2E}\right), \tag{2.7}$$

where $\mathcal{V}_n = {}_{\rm art}\langle E|V_{\rm art}|b_n\rangle$. This gives the inelastic-scattering cross section

$$\sigma_{\rm inel} = \frac{4\pi g_s}{k^2}|\pi\left(\mathcal{V}_1 A_{1E} + \mathcal{V}_2 A_{2E}\right)|^2, \tag{2.8}$$

where $g_s = 1(2)$ for two distinguishable (indistinguishable) atoms. The atom-loss rate is given by $K_{\rm loss} = \langle v_{\rm rel}\sigma_{\rm inel}\rangle$ where $\langle\cdots\rangle$ implies thermal averaging over a Maxwell–Boltzmann distribution of the relative velocity $v_{\rm rel} = \hbar k/\mu$ with k being the relative wave number. Clearly, $\sigma_{\rm inel}$ or $K_{\rm loss}$ will vanish if $\mathcal{V}_1 A_{1E} = -\mathcal{V}_2 A_{2E}$, meaning

$$\frac{A_{1E}}{A_{2E}} = -\frac{\mathcal{V}_2}{\mathcal{V}_1} = -\sqrt{\frac{\gamma_2}{\gamma_1}} \tag{2.9}$$

is the condition for the onset of an excited molecular dark state that is protected against spontaneous emission. This condition can be fulfilled by suitably adjusting the relative intensity and phase between the two lasers, and the two detuning parameters Δ_1 and Δ_2.

The elastic-scattering amplitude can be obtained from asymptotic analysis of the dressed wave function $\psi_E(\mathbf{r}) = \langle\mathbf{r}|\psi_E\rangle$, where $\mathbf{r}$ stands for the relative position vector of the two atoms. This can be conveniently done by partial-wave expansion as done in detail in Ref. [19]. The scattering properties of low-lying partial waves $\ell = 0$ (s wave), $\ell = 1$ (p wave), or $\ell = 2$ (d wave) can be optically manipulated by this two-laser–OFR method. Which partial-wave will be most influenced by this method depends on the rotational quantum numbers of the two excited bound states and the temperature of the atomic cloud. While ultracold temperatures in the Wigner-threshold-law regime are most suitable for manipulating s-wave collisions, temperatures slightly higher than the Wigner-threshold-law regime or temperatures near a shape resonance are appropriate for controlling higher-partial-wave collisional properties. As an illustration we analyze the manipulation of p-wave-scattering properties of ^{171}Yb atoms with two-laser OFR in the next section.

III. TWO-LASER p-WAVE OPTICAL FESHBACH RESONANCE IN ^{171}Yb ATOMS

For the bound states $|b_1\rangle$ and $|b_2\rangle$, we choose purely-long-range (PRL) molecular states of $^{171}Yb_2$. These states are fundamentally different from the usual molecular bound states on several counts. First, these states are formed due to an interplay between resonant dipole-dipole and spin-orbit or hyperfine interactions in the excited atomic states. Second, their equilibrium position lies at a large separation well beyond the chemically interactive region of the overlap between the electron clouds of the two atoms. Third, the constituent atoms retain most of their atomic characters. Fourth, the potentials supporting such states are usually very shallow, allowing only a few vibrational levels to exist. Predicted about 35 years ago [35,36], these states were recently observed experimentally in alkali-metal [37–42], metastable-helium [43], and fermionic-ytterbium [44] atoms with PA spectroscopy. These states will be particularly useful for the optical manipulation of p or higher partial-wave atom-atom interactions. One of the major obstacles to higher-partial-wave OFR stems from the fact that the partial-wave centrifugal barrier is too high for the low-energy scattering wave function to be appreciable in the short-range region. With PLR states being used for OFR, PA transitions need not take place inside the barrier, opening up a new scope for higher-partial-wave OFR. The fact that the photoassociative atom loss mostly occurs in the relatively-short-range region makes PLR states a better choice for OFR in order to mitigate the loss.

In the case of ^{171}Yb atoms, PLR bound states are formed due to an interplay between resonant dipole-dipole and hyperfine interactions. The PLR potential of $^{171}Yb_2$ of the state $^1S_0 + {}^3P_1$ is obtained [44] by diagonalizing the adiabatic Hamiltonian

$$H_{\rm adia} = \frac{\mathbf{d}_1\cdot\mathbf{d}_2 - 3d_{1z}d_{2z}}{R^3} + a\left(\mathbf{i}_1\cdot\mathbf{j}_1 + \mathbf{i}_2\cdot\mathbf{j}_2\right) - \frac{C_6}{R^6}, \tag{3.1}$$

where $\mathbf{d}_n$, d_{nz}, $\mathbf{j_n}$, and $\mathbf{i_n}$ denote the dipole moment of the atomic transition $^1S_0 \to {}^3P_1$, z component of the dipole moment and electronic and nuclear-spin angular momenta, respectively, of the nth (=1,2) atom. Here, the parameters $a = 3957$ MHz, $C_6 = 2810$ a.u., and the magnitude of the transition dipole moment $d = 0.311$ a.u. The axial projection Ω of of the total electronic angular momentum $\mathbf{J} = \mathbf{j}_1 + \mathbf{j}_2$ is not a good quantum number. The total nuclear-spin angular momentum is $\mathbf{I} = \mathbf{i}_1 + \mathbf{i}_2$. The axial projection Φ of the total angular momentum $\mathbf{F} = \mathbf{J} + \mathbf{I}$ is a good quantum number. Furthermore, when we include the rotation of the internuclear axis described by the partial wave ℓ, the good quantum numbers are $\mathbf{T} = \mathbf{F} + \vec{\ell}$ and its projection M_T on the space-fixed axis. Now, an effective excited potential is

$$V_e(r) = V_{\rm PLR}(r) + \frac{\hbar^2 T_e\left[T_e + 1\right] + \langle F^2\rangle - 2\Phi^2}{2\mu r^2}, \tag{3.2}$$

where $V_{\rm PLR}(r)$ is the PLR potential obtained by diagonalizing Eq. (3.1), μ is the reduced mass, and T_e represents the rotational quantum number of the excited molecular state. The PLR potential that is accessible the p-wave ground-state scattering state via PA has depth of about 750 MHz and an equilibrium separation at 75 Bohr radii [44]. The ground-state potential is

$$V_g = \frac{C_{12}}{r^{12}} - \frac{C_6}{r^6} - \frac{C_8}{r^8} + \frac{\ell\left(\ell+1\right)}{2\mu r^2}, \tag{3.3}$$

where $C_{12} = 1.034\,09\times10^9$ a.u., $C_8 = 1.93\times10^5$ a.u., and $C_6 = 1931.7$ a.u. [17,45]. Ground-state ^{171}Yb has nuclear spin $i = \frac{1}{2}$ with no electronic spin. The ground-state collision in the s (p) partial-wave is characterized by the total nuclear spin $I = 0$ (1) due to the antisymmetry of the total wave function. For molecular transitions, ground and excited states must have opposite parity. The selection rule is $\Delta T = 0,1$ with $T = 0 \to T = 0$ being forbidden. For $\Phi_e \neq 0$ all T_e are allowed. For the $\Phi_e = 0$ state, only odd or even T_e are allowed [44,46–48]. For p waves, we use a 0^- PLR state, so only odd T_e are allowed.

Let us consider two PLR excited bound states of $^{171}Yb_2$ represented by $|b_\nu\rangle \equiv |T_e M_{T_e}\rangle_\nu$, where T_e is the rotational quantum number, M_{T_e} denotes its projection along the z axis of the laboratory frame, and ν (=1,2) is the vibrational quantum

number. As shown in Fig. 1, two OFR lasers L_1 and L_2 are used to induce photoassociative dipole coupling between the ground continuum state and the excited bound states with vibrational quantum numbers $v = 1$ and $v = 2$, respectively. Both the bound states have the same rotational quantum numbers either $T_e = 1$ or $T_e = 3$. Let the internal (rotational) state of the two ground-state atoms in the molecular basis be denoted by $|T_g M_{T_g}\rangle$.

The dressed continuum of Eq. (2.1) can be derived following the method given in the Appendix A of Ref. [19]. It can be most conveniently done by using the expansion in terms of molecular-angular-momentum basis functions or spherical harmonics. However, instead of the $|\ell, m_\ell\rangle$ basis for the ground state, we use the $|T_g, M_{T_g}\rangle$ basis for the present context.

The photoassociative loss of atoms is governed by the equation $\dot{n} = K_{\rm loss} n^2$ where n is the atomic number density. Assuming a uniform number density $\bar{n}$, the number of atoms remaining after the simultaneous action of both the lasers for a duration of τ is given by

$$N_{\rm remain} = \frac{N_0}{1 + \bar{n} K_{\rm loss} \tau}, \tag{3.4}$$

where N_0 is the initial number of atoms.

Elastic-scattering cross section

For the geometry and polarizations chosen for the two laser beams as schematically shown in Fig. 2, it is clear that the optical transitions couple ground and excited magnetic sublevels $M_{T_1} = M_{T_2} = M_{T_g}$. We take $T_1 = T_2 = T_e$.

The asymptotic form of $\psi_E(\mathbf{r})$ is given by

$$\psi_E(\mathbf{r} \to \infty) \sim r^{-1} \sum_{M_{T_g}, M'_{T_g}} \psi^{T_g M'_{T_g}}_{T_g M_{T_g}}(r)\, Y^*_{T_g, M'_{T_g}}(\hat{k}) \langle \hat{r} | T_g M_{T_g} \rangle, \tag{3.5}$$

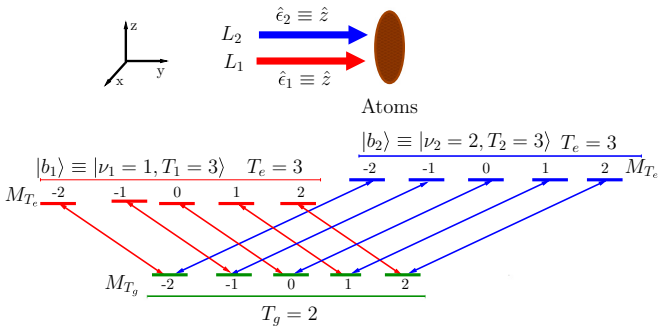

FIG. 2. (Color online) Schematic diagram showing how two lasers couple different molecular magnetic sublevels of ground and excited states of ^{171}Yb atoms. Both lasers are linearly polarized along the z axis. A pair of photons—one from the L_1 laser (red) and the other from the L_2 (blue) laser—couple a particular ground-state magnetic sublevel M_{T_g} with two excited states having same angular momenta $T_e = 3$ and $M_{T_e} = M_{T_g}$, where M_{T_g} can take any of the five values from -2 to 2. Since the angular parts of the amplitudes for each such pair of transitions are the same, the magnitudes of the two transition amplitudes can be made equal by suitably adjusting the relative intensity of the two lasers. The phase of the two transition amplitudes is opposite due to the opposite vibrational parity of the two excited states.

where

$$\psi^{T_g M'_{T_g}}_{T_g M_{T_g}}(r)\, \langle \hat{r} | T_g M_{T_g} \rangle = \sum_{\substack{m_l, m_I, \\ m_l + m_I = M_T}} C^{T_g M_{T_g}}_{l m_l I m_I} \langle \hat{r} | l m_l I m_I, T_g M_{T_g} \rangle \left[\sin\left(kr - \frac{l\pi}{2} - \eta \right) - \pi F^{T_g M'_{T_g}}_{T_g M_{T_g}}(E, E') \exp\left\{ i \left(kr - \frac{l\pi}{2} - \eta \right) \right\} \right], \tag{3.6}$$

where η is the background (in the absence of lasers) phase shift and $C^{T_g M_{T_g}}_{l m_l I m_I}$ is the Clebsch–Gordan coefficient. Comparing this with Eq. (1) and using the expansion $C_{E'} \equiv \sum_{M_{T_g}, M'_{T_g}} C^{T_g M'_{T_g}}_{E', T_g M_{T_g}} Y^*_{T_g M'_{T_g}}(\hat{k})$, we can relate $C^{T_g M'_{T_g}}_{E', T_g M_{T_g}} \langle r | E' \rangle_g \equiv \psi^{T_g M'_{T_g}}_{T_g M_{T_g}}(r)$. The $\mathcal{T}$ matrix element is given by

$$\mathcal{T}_{T M_T, T M'_T} = -e^{i\eta} \sin\eta\, \delta_{m_l m'_l} \delta_{m_I m'_I} + \pi F^{T_g M'_{T_g}}_{T_g M_{T_g}} e^{2i\eta}. \tag{3.7}$$

The elastic-scattering cross section is

$$\sigma_{\rm el} = \frac{4\pi g_s}{k^2} \sum_{M_T, M'_{T_g}} \left| \mathcal{T}_{T_g M_{T_g}, T_g M'_{T_g}} \right|^2. \tag{3.8}$$

By using the expansion

$$A_{\nu E} = \sum_{T_g, M'_{T_g}} A^{T_g M'_{T_g}}_{\nu E}(M_{T_e}) Y^*_{T_g M'_{T_g}}(\hat{k}),$$

we have [19]

$$F^{T_g M'_{T_g}}_{T_g M_{T_g}} = \sum_{\nu, M_{T_e}} A^{T_g M'_{T_g}}_{\nu E} \Lambda^{\nu, T_e M_{T_e}}_{T_g M_{T_g}}(E). \tag{3.9}$$

Here, $\Lambda^{\nu, T_e M_{T_e}}_{T_g M_{T_g}}(E)$ is the amplitude for the optical transition $|T_e, M_{T_e}\rangle_\nu \to |E, T_g M_{T_g}\rangle$ due to the L_ν laser, where $|E, T_g M_{T_g}\rangle$ represents the unperturbed (laser-free) scattering state for (T_g, M_{T_g}) quantum numbers. Explicitly,

$$A^{T_g M'_{T_g}}_{\nu E}(M_{T_e}) = D^{-1}_\nu \left[\left\{ \Lambda^{\nu, T_e M_{T_e}}_{T_g M'_{T_g}}(E) \right\}^* + \mathcal{L}^{\nu'}_\nu \right], \quad \nu' \neq \nu, \tag{3.10}$$

where $D_\nu = \zeta_\nu + i\mathcal{J}_\nu/2$ with $\mathcal{J}_\nu = \Gamma_\nu + \Gamma_{\nu\nu'} + \gamma_\nu$, $\zeta_\nu = E + \hbar\Delta_\nu - (E_\nu + E^{\rm shift}_\nu + E^{\rm shift}_{\nu\nu'})$. Here,

$$\mathcal{L}^{\nu'}_\nu = \xi^{-1}_{\nu'} \mathcal{K}_{\nu\nu'}, \tag{3.11}$$

with $\xi_\nu(E) = E + \hbar\Delta_\nu - (E_\nu + E^{\rm shift}_\nu) + i\Gamma_\nu/2$, and

$$\mathcal{K}_{\nu\nu'} = \left(\mathcal{V}_{\nu\nu'} - i\tfrac{1}{2}\hbar\mathcal{G}_{\nu\nu'} \right) \tag{3.12}$$

is the cross coupling between two excited bound states induced by the two lasers, where

$$\mathcal{V}_{\nu\nu'} = \sum_{T M_T} \mathcal{P} \int \frac{\Lambda^{\nu, T_e M_{T_e}}_{T_g M_{T_g}}(E') \left\{ \Lambda^{\nu', T_e M_{T_e}}_{T_g M_{T_g}}(E') \right\}^*}{E - E'} dE', \tag{3.13}$$

$$\mathcal{G}_{\nu\nu'} = \frac{2\pi}{\hbar} \sum_{T M_T} \Lambda^{\nu, T_e M_{T_e}}_{T_g M_{T_g}}(E) \left\{ \Lambda^{\nu', T_e M_{T_e}}_{T_g M_{T_g}}(E) \right\}^*. \tag{3.14}$$

The stimulated linewidth of the νth bound state due to the νth laser only is

$$\Gamma_\nu(E) = \frac{2\pi}{\hbar}\sum_{M_{T_g}} \left|\Lambda^{\nu,T_eM_{T_e}}_{T_gM_{T_g}}(E')\right|^2, \tag{3.15}$$

and the corresponding light shift is

$$E^{\text{shift}}_\nu = \sum_{M_T}\mathcal{P}\int \frac{\Lambda^{\nu,T_eM_{T_e}}_{T_gM_{T_g}}(E')\left\{\Lambda^{\nu,T_eM_{T_e}}_{T_gM_{T_g}}(E')\right\}^*}{E-E'}dE'. \tag{3.16}$$

The terms that arise due to the cross coupling $\mathcal{K}_{\nu\nu'}$ are

$$E^{\text{shift}}_{\nu\nu'} = \text{Re}\left[\xi^{-1}_{\nu'}\mathcal{K}_{\nu\nu'}\mathcal{K}_{\nu'n}\right], \tag{3.17}$$

$$\Gamma_{\nu\nu'} = -2\text{Im}\left[\xi^{-1}_{\nu'}\mathcal{K}_{\nu\nu'}\mathcal{K}_{\nu'\nu}\right]. \tag{3.18}$$

IV. RESULTS AND DISCUSSIONS

For numerical illustration, we consider that the two OFR lasers L_1 and L_2 couple $T_g = 2$ to two PLR vibrational states $\nu = 1$ (b_1) and $\nu = 2$ (b_2), respectively, with same $T_e = 3$. As discussed in the previous section, from symmetry considerations, the PLR states chosen will be accessible only from odd partial waves (odd ℓ) and nuclear spin triplets ($I = 1$). As per the selection rule $\Delta T = 0,1$, the excited rotational state $T_e = 3$ will be accessible from the ground $T_g = 2$ or $T_g = 4$, which means from $\ell = 1$ or $\ell = 3$. We assume that the contributions from $\ell = 3$ is negligible due to low temperature. Furthermore, we select laser detunings and intensities such that the optical couplings to the levels $T_1 = T_2 = 1$ are negligible. We can thus restrict our study to $T_g = 2$ only. These two states have the binding energies $E_{b_1} = -355.4$ MHz and $E_{b_2} = -212.4$ MHz measured from the threshold of the excited potential. The laser irradiation time is taken to be 30 ms, and the average atomic density $\bar{n} = 2\times10^{13}$ cm^{-3} [16,49], temperature is 8 μK, and the initial atom number $N_0 = 1.7\times10^5$. Spontaneous linewidths of the bound states are $\gamma_1 = \gamma_2 = 2\pi\times364$ kHz [16,49].

Figures 3(a)–3(d) display the number N_{remain} of atoms remaining and the PA loss rate K_{loss} as a function of detuning of the first laser, $\Delta_1 = \omega_{L_1} - \omega_A$, from the atomic transition frequency ω_A (asymptote of the PLR potential) for different intensities of the two lasers. In Figs. 3(a) and 3(b), the first laser intensity is fixed in the intermediate coupling regime ($\Gamma_1 \leqslant \gamma$) while the intensity of the second laser is set for the strong-coupling regime ($\Gamma_2 > \gamma$). For Fig. 3(c), the intensities of both lasers are in the strong-coupling regimes ($\Gamma_1 \gg \gamma$, $\Gamma_2 \gg \gamma$). K_{loss} (dashed curves) in Figs. 3(a)–3(d) exhibits a prominent minimum, the values of K_{loss} at the minima being about 3.8×10^{-14} cm^3/s, 7.0×10^{-15} cm^3/s, 1.5×10^{-16} cm^3/s, and 2.96×10^{-16} cm^3/s, respectively. Let $\Delta_{1,\text{min}}$ be the value of Δ_1 at which the minimum occurs. N_{remain} as a function of Δ_1 exhibits complementary behavior to that of K_{loss}, attaining the maximum exactly at $\Delta_{1,\text{min}}$. The value N_{remain} at $\Delta_{1,\text{min}}$ is nearly equal to N_0, implying that the loss of atoms is negligible at $\Delta_{1,\text{min}}$. This occurs due to the formation of a molecular dark state, leading to destructive quantum interference between

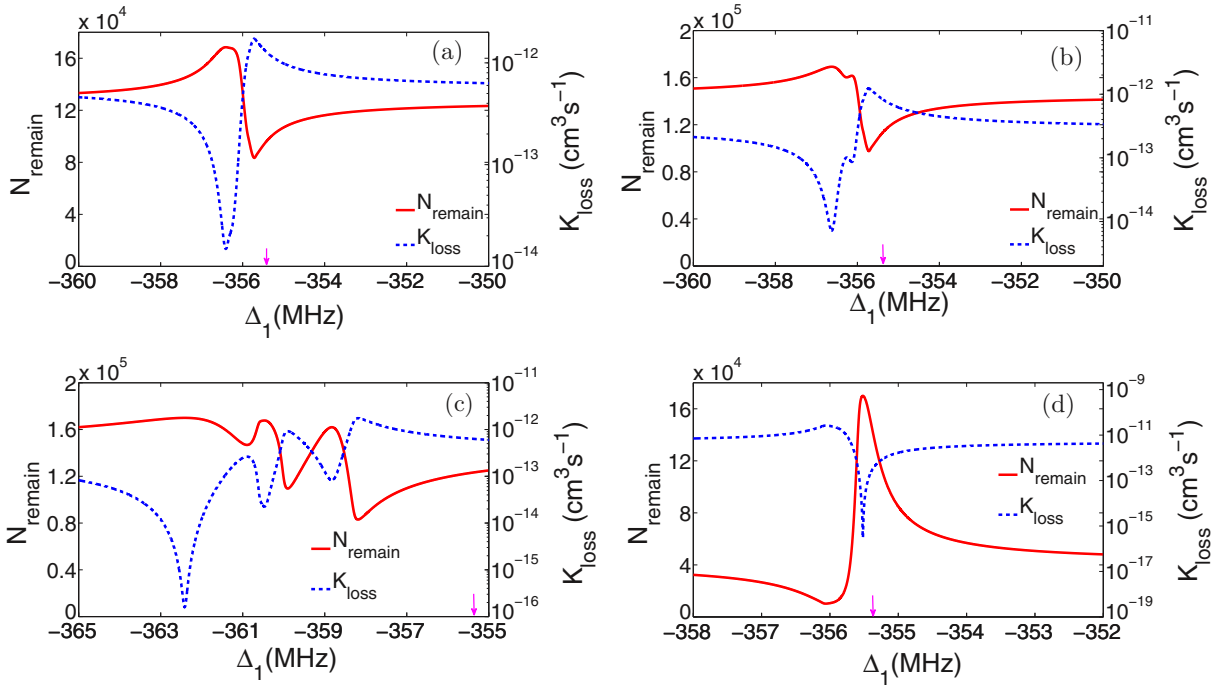

FIG. 3. (Color online) Number of atoms N_{remain} (solid curves) remaining in the trap after the two OFR lasers have acted for 30 ms and PA rate K_{loss} (dashed curves) in units of cm^3/s are plotted against the detuning Δ_1 (in MHz) of the first laser from the atomic-transition frequency at temperature $T = 8$ μK for different laser intensities: (a) $I_1 = 1$ W/cm^2 ($\Gamma_1 = 212.9$ kHz) and $I_2 = 10$ W/cm^2 ($\Gamma_2 = 4.3$ MHz), (b) $I_1 = 1$ W/cm^2 ($\Gamma_1 = 212.9$ kHz) and $I_2 = 20$ W/cm^2 ($\Gamma_2 = 8.6$ MHz), (c) $I_1 = 10$ W/cm^2 ($\Gamma_1 = 2.1$ MHz) and $I_2 = 20$ W/cm^2 ($\Gamma_2 = 8.6$ MHz), (d) $I_1 = 0.2$ W/cm^2 ($\Gamma_1 = 106$ kHz) and $I_2 = 0.1$ W/cm^2 ($\Gamma_2 = 43$ kHz). The other parameters are $\delta_2 = 0$ and laser phase difference $\theta = 0$. The arrow indicates the binding energy $E_{b_1} = -355.4$ MHz of the unperturbed bound state $|b_1\rangle$.

TABLE I. The values of $E_{12}^{\rm shift}(M_T)$ in MHz are shown for the laser intensities used in Fig. 3 with $\delta_2 = 0$.

I_1 W/cm^2	I_2 W/cm^2	$E_{12}^{\rm shift}$ $(M_T = 0)$	$E_{12}^{\rm shift}$ $(M_T = 1)$	$E_{12}^{\rm shift}$ $(M_T = 2)$
1	10	1.09	0.975	0.60
1	20	1.10	0.980	0.610
10	20	11.03	9.8	6.10
0.2	0.1	0.117	0.098	0.047

spontaneous emission transition pathways. The fact that the spectra for both $K_{\rm loss}$ and $N_{\rm remain}$ in Fig. 3 are asymmetric with a prominent minimum and a maximum is indicative of the occurrence of quantum interference. In case of one-laser OFR in the weak-coupling regime ($\Gamma \ll \gamma$), the spectra have symmetric Lorentzian shape. We notice that $\Delta_{1,\rm min}$ exhibits shifts towards the lower values of $\omega_{\rm L_1}$ as we move from Fig. 3(a) to Fig. 3(c). The increasing redshifts due to increasing laser intensity I_1 are consistent with the calculated light shifts. Light shift $E_{\nu_n,M_{T_n}}^{\rm shift}$ of $|b_n\rangle$ due to the $\rm L_n$ laser only is proportional to the laser intensity I_n and does not depend on the detunings. In contrast, $E_{\nu\nu'}^{\rm shift}$ depends on both laser intensities and the detuning $\Delta\nu'$. We found $E_{\nu_1,M_{T_1}=0}^{\rm shift}/I_1 = -1.62$ MHz cm^2/W, $E_{\nu_1,M_{T_1}=1}^{\rm shift}/I_1 = -1.44$ MHz cm^2/W, $E_{\nu_1,M_{T_1}=2}^{\rm shift}/I_1 = -0.904$ MHz cm^2/W, and $E_{\nu_1,M_{T_2}=0}^{\rm shift}/I_2 = -1.82$ MHz cm^2/W, $E_{\nu_1,M_{T_2}=1}^{\rm shift}/I_2 = -1.61$ MHz cm^2/W, $E_{\nu_1,M_{T_2}=2}^{\rm shift}/I_2 = -1.00$ MHz cm^2/W. The calculated values of $E_{12}^{\rm shift}$ and $E_{21}^{\rm shift}$ are given in the Tables I and II, respectively.

From Figs. 3(a)–3(c), we further notice that the width of the dip in $K_{\rm loss}$ or equivalently the width of the maximum in $N_{\rm remain}$ increases as we move from Fig. 3(a) to Fig. 3(c). This means that the strong-coupling regimes with a molecular dark resonance are robust for efficient manipulation of atom-atom interactions. The oscillations in Fig. 3 result from the laser-induced coherence between the two excited bound states described by the term $\mathscr{L}_{\nu}^{\nu'}$. This laser-induced coherence is important in the strong-coupling regimes because it comes into play due to nonlinear effects. One photon from the $\rm L_1$ laser excites the bound state $|b_1\rangle$ which then emits another photon by stimulated emission. When this absorption-emission cycle is followed by the excitation of the other bound state $|b_2\rangle$ by one photon from $\rm L_2$ laser, we have the coherence $\mathscr{L}_{\nu=2}^{\nu'=1}$. The maximum in $N_{\rm remain}$ vs Δ_1 and the spectral asymmetry also appear in weak-coupling regimes for both lasers, as shown in Fig. 3(d). At collision energy $E = 8$ μK the square of

TABLE II. The values of $E_{21}^{\rm shift}(M_T)$ in MHz are shown for $\Delta_1 = \Delta_{1,\rm min}$.

I_1 W/cm^2	I_2 W/cm^2	$E_{21}^{\rm shift}$ $(M_T = 0)$	$E_{21}^{\rm shift}$ $(M_T = 1)$	$E_{21}^{\rm shift}$ $(M_T = 2)$
1	10	12.58	38.56	−47.7
1	20	25.66	82.43	−77.72
10	20	43.49	41.52	55.90
0.2	0.1	0.102	0.089	0.050

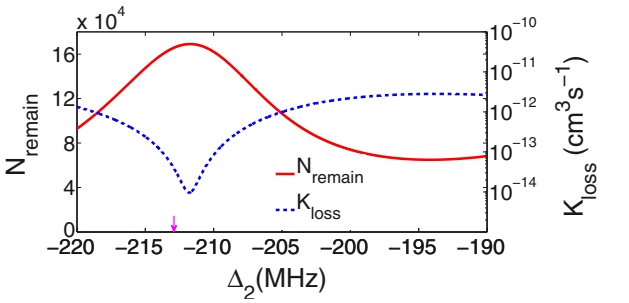

FIG. 4. (Color online) Same as in Fig. 3(b) but as a function of Δ_2 at $\Delta_1 = \Delta_{1,\rm min}$.

the Franck–Condon overlap integral for the transition to $|b_2\rangle$ is about two times larger than that to $|b_1\rangle$. Therefore, if we fix the intensity of laser $\rm L_1$ at half the intensity of laser $\rm L_2$, we expect that the two free-bound transition amplitudes with $M_{T_g} = M_{T_e}$ will be almost same. Then, in the weak-coupling regimes, we would expect the maximum in $N_{\rm remain}$ to occur at or near the energy of the unperturbed bound state $|b_1\rangle$ if the maximum arises due to the dark state. In fact, the solid curve in Fig. 3(d) has the maximum near the binding energy of $|b_1\rangle$.

Keeping the value of Δ_1 fixed at $\Delta_{1,\rm min}$, which happens to be $\tilde{\delta}_1 \simeq 0$, we plot $K_{\rm loss}$ and $N_{\rm remain}$ as a function of Δ_2 in Fig. 4. for the parameters as in Fig. 3(b). This shows that $K_{\rm loss}$ has a broad minimum when Δ_2 is tuned near the resonance to $|b_2\rangle$. The loss of atoms is almost nil for the parameters at which the minimum in $K_{\rm loss}$ occurs.

We next show the elastic-scattering cross section $\sigma_{\rm el}$ as a function of Δ_1 and compare it with the inelastic one $\sigma_{\rm inel}$ in Fig. 5, keeping other parameters fixed as in Fig. 3(b). $\sigma_{\rm el}$ is six orders of magnitude larger at and near $\Delta_{1,\rm min}$ where the minimum of $\sigma_{\rm inel}$ occurs due to the dark state. Note that the background (in the absence of OFR) elastic cross section is negligible ($\sim 10^{-19}$ cm^2). We found that $\sigma_{\rm el}$ and $\sigma_{\rm inel}$ are of comparable magnitudes in the weak-coupling regimes.

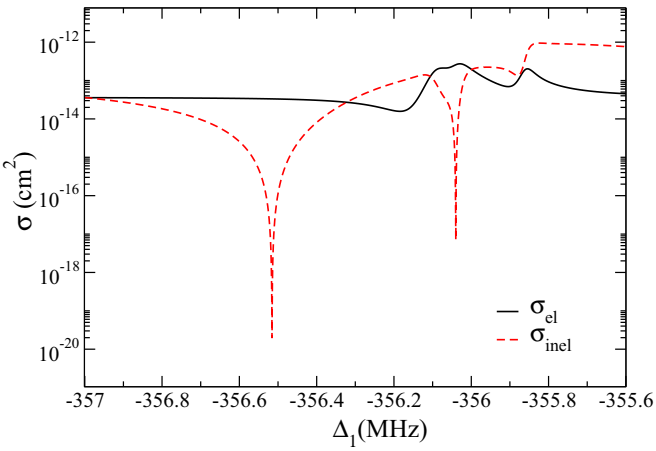

FIG. 5. (Color online) $\sigma_{\rm el}$ and $\sigma_{\rm inel}$ plotted as a function of Δ_1 for collision energy $E = 8$ μK. All other parameters are same as in Fig. 3(b).

V. CONCLUSION

In conclusion, we demonstrated highly efficient manipulation of p-wave interactions between fermionic ^{171}Yb atoms with an optical method that uses two lasers in the strong-coupling regime. This method relies on creating a molecular dark state in the electronically excited potential, leading to the inhibition of photoassociative atom loss. It is possible when two excited molecular bound states coupled to the continuum of scattering states by the two lasers have the same rotational quantum number; and all pairs of excited sublevels having the same magnetic quantum number are coupled a ground-state sublevel by the two lasers, as schematically depicted in Fig. 2. This ensures the cancellations of spontaneous emission from all the excited sublevels when the conditions for the formation of the dark state are fulfilled. The efficiency of our method may be characterized by a number of parameters: (1) the ratio $N_{\rm remain}/N_0$ of the number $N_{\rm remain}$ of atoms remaining to the initial number N_0, (2) the ratio $\sigma_{\rm el}/\sigma_{\rm inel}$ of the elastic- to inelastic-scattering cross sections, and (3) the ratio of the width of the dip in atom-loss rate to the spontaneous linewidth. When the conditions for dark state are satisfied in the strong-coupling regimes for both the lasers, we have the results $N_{\rm remain}/N_0 \simeq 1$, $\sigma_{\rm el}/\sigma_{\rm inel}\frac{a}{b} \sim 10^4$–$10^6$ and the ratio between the two widths can be much larger than 1. Considering the velocity of the atoms to be a few cm/s and the number density $\sim 10^{13}$ cm^{-3}, we find an elastic rate ~ 1 s^{-1} while the inelastic rate $\sim 10^{-5}$ s^{-1}. These numbers indicate that it is possible to manipulate atom-atom interactions efficiently by the optical method presented in this paper.

ACKNOWLEDGMENTS

We are thankful to Yoshiro Takahashi and Katsunari Enomoto for sending us a numerical code to calculate PLR potentials.

[1] E. Tiesinga, B. J. Verhaar, and H. T. C. Stoof, Phys. Rev. A **47**, 4114 (1993).
[2] S. Inouye, M. R. Andrews, J. Stenger, H.-J. Miesner, D. M. Stamper-Kurn, and W. Ketterle, Nature (London) **392**, 151 (1998).
[3] J. L. Roberts, N. R. Claussen, James P. Burke, Jr., Chris H. Greene, E. A. Cornell, and C. E. Wieman, Phys. Rev. Lett. **81**, 5109 (1998).
[4] J. K. Chin, D. E. Miller, Y. Liu, C. Stan, W. Setiawan, C. Sanner, K. Xu, and W. Ketterle, Nature (London) **443**, 961 (2006).
[5] C. A. Regal, C. Ticknor, J. L. Bohn, and D. S. Jin, Phys. Rev. Lett. **90**, 053201 (2003).
[6] J. Zhang, E. G. M. van Kempen, T. Bourdel, L. Khaykovich, J. Cubizolles, F. Chevy, M. Teichmann, L. Tarruell, S. J. J. M. F. Kokkelmans, and C. Salomon, Phys. Rev. A **70**, 030702(R) (2004).
[7] C. H. Schunck, M. W. Zwierlein, C. A. Stan, S. M. F. Raupach, W. Ketterle, A. Simoni, E. Tiesinga, C. J. Williams, and P. S. Julienne, Phys. Rev. A **71**, 045601 (2005).
[8] F. Chevy, E. G. M. van Kempen, T. Bourdel, J. Zhang, L. Khaykovich, M. Teichmann, L. Tarruell, S. J. J. M. F. Kokkelmans, and C. Salomon, Phys. Rev. A **71**, 062710 (2005).
[9] Preg Zhang, Pascal Naidon, and Masahito Ueda, Phys. Rev. A **82**, 062712 (2010).
[10] J. P. Gaebler, J. T. Stewart, J. L. Bohn, and D. S. Jin, Phys. Rev. Lett. **98**, 200403 (2007).
[11] K. B. Gubbels and H. T. C. Stoof, Phys. Rev. Lett. **99**, 190406 (2007).
[12] P. O. Fedichev, Yu. Kagan, G. V. Shlyapnikov, and J. T. M. Walraven, Phys. Rev. Lett. **77**, 2913 (1996).
[13] F. K. Fatemi, K. M. Jones, and P. D. Lett, Phys. Rev. Lett. **85**, 4462 (2000).
[14] M. Theis, G. Thalhammer, K. Winkler, M. Hellwig, G. Ruff, R. Grimm, and J. H. Denschlag, Phys. Rev. Lett. **93**, 123001 (2004).
[15] G. Thalhammer, M. Theis, K. Winkler, R. Grimm, and J. H. Denschlag, Phys. Rev. A **71**, 033403 (2005).
[16] R. Yamazaki, S. Taie, S. Sugawa, K. Enomoto, and Y. Takahashi, Phys. Rev. A **87**, 010704(R) (2013).
[17] K. Goyal, I. Reichenbach, and I. Deutsch, Phys. Rev. A **82**, 062704 (2010).
[18] B. Deb and J. Hazra, Phys. Rev. Lett. **103**, 023201 (2009).
[19] B. Deb, Phys. Rev. A **86**, 063407 (2012).
[20] G. Alzetta, A. Gozzini, L. Moi, and G. Orriols, Nuovo Cimento B **36**, 5 (1976).
[21] E. Arimondo, in *Progress in Optics*, edited by E. Wolf (Elsevier, Amsterdam, 1996), Vol. 35, p. 257.
[22] C. Cohen-Tannoudji, J. Dupont-Roc, and G. Grynberg, *Atom-Photon Interactions: Basic Processes and Applications* (Wiley, New York, 1992).
[23] A. Aspect, E. Arimondo, R. Kaiser, N. Vansteenkiste, and C. Cohen-Tannoudji, Phys. Rev. Lett. **61**, 826 (1988).
[24] A. Aspect, E. Arimondo, R. Kaiser, N. Vansteenkiste, and C. Cohen-Tannoudji, J. Opt. Soc. Am. B **6**, 2112 (1989).
[25] J. R. Kuklinski, U. Gaubatz, F. T. Hioe, and K. Bergmann, Phys. Rev. A **40**, 6741(R) (1989).
[26] N. V. Vitanov, Adv. At. Mol. Phys. **46**, 55 (2001).
[27] K. Bergmann, H. Theuer, and B. W. Shore, Rev. Mod. Phys. **70**, 1003 (1998).
[28] S. E. Harris, Phys. Today **50**, 36 (1997).
[29] L. V. Hau, S. E. Harris, Z. Dutton, and C. H. Behroozi, Nature (London) **397**, 594 (1999).
[30] R. Ciurylo, E. Tiesinga, and P. S. Julienne, Phys. Rev. A **71**, 030701(R) (2005).
[31] K. Enomoto, K. Kasa, M. Kitagawa, and Y. Takahashi, Phys. Rev. Lett. **101**, 203201 (2008).
[32] S. Das, A. Rakshit, and B. Deb, Phys. Rev. A **85**, 011401(R) (2012).
[33] A. Rakshit, S. Ghosh, and B. Deb, J. Phys. B: At. Mol. Phys. **47**, 115303 (2014).
[34] John L. Bohn and P. S. Julienne, Phys. Rev. A **60**, 414 (1999).
[35] M. Movre and G. Pichler, J. Phys. B: At. Mol. Phys. **10**, 2631 (1977).

[36] W. C. Stwalley, Y. H. Uang, and G. Pichler, Phys. Rev. Lett. **41**, 1164 (1978).
[37] R. A. Cline, J. D. Miller, and D. J. Heinzen, Phys. Rev. Lett. **73**, 632 (1994).
[38] L. P. Ratliff, M. E. Wagshul, P. D. Lett, S. L. Rolston, and W. D. Phillips, J. Chem. Phys. **101**, 2638 (1994).
[39] H. Wang, P. L. Gould, and W. C. Stwalley, Phys. Rev. A **53**, R1216(R) (1996).
[40] A. Fioretti, D. Comparat, A. Crubellier, O. Dulieu, F. Masnou-Seeuws, and P. Pillet, Phys. Rev. Lett. **80**, 4402 (1998).
[41] X. Wang, H. Wang, P. L. Gould, W. C. Stwalley, E. Tiesinga, and P. S. Julienne, Phys. Rev. A **57**, 4600 (1998).
[42] D. Comparat, C. Drag, B. Laburthe Tolra, A. Fioretti, P. Pillet, A. Crubellier, O. Dulieu, and F. Masnou-Seeuws, Eur. Phys. J. D **11**, 59 (2000).
[43] J. Leonard, M. Walhout, A. P. Mosk, T. Muller, M. Leduc, and C. Cohen-Tannoudji, Phys. Rev. Lett. **91**, 073203 (2003).
[44] K. Enomoto, M. Kitagawa, S. Tojo, and Y. Takahashi, Phys. Rev. Lett. **100**, 123001 (2008).
[45] M. Kitagawa, K. Enomoto, K. Kasa, Y. Takahashi, R. Ciurylo, P. Naidon, and P. S. Julienne, Phys. Rev. A **77**, 012719 (2008).
[46] E. R. I. Abraham, W. I. McAlexander, H. T. C. Stoof, and R. G. Hulet, Phys. Rev. A **53**, 3092 (1996).
[47] E. Tiesinga, K. M. Jones, P. D. Lett, U. Volz, C. J. Williams, and P. S. Julienne, Phys. Rev. A **71**, 052703 (2005).
[48] J. Brown and A. Carrington, *Rotational Spectroscopy of Diatomic Molecules* (Cambridge University Press, Cambridge, 2003).
[49] K. Enomoto, M. Kitagawa, K. Kasa, S. Tojo, and Y. Takahashi, Phys. Rev. Lett. **98**, 203201 (2007).